Fully-coupled 3D modelling of magmatic dike Propagation – finite pulse release from a point source

Andreas Möri[1,2], Brice Lecampion[1], Haseeb Zia[1]

[1]Ecole polytéchnique fédérale de Lausanne, Switzerland

- **When does a finite pulse release transition into a dike propagation?**
- **What is the 3D shape of the buoyant fracture?**

[2]Correspondence to: andreas.mori@epfl.ch

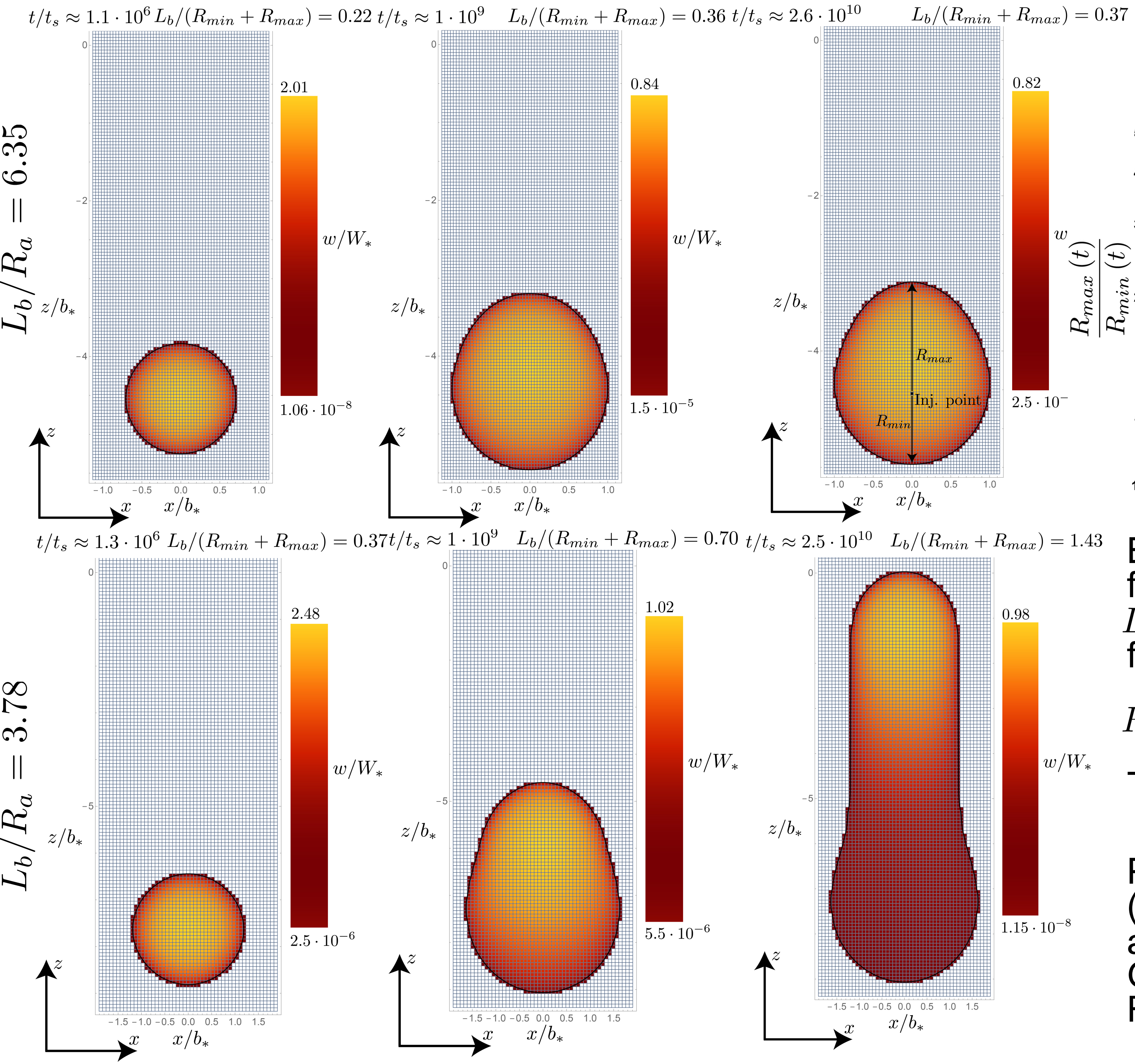

Radial to buoyant

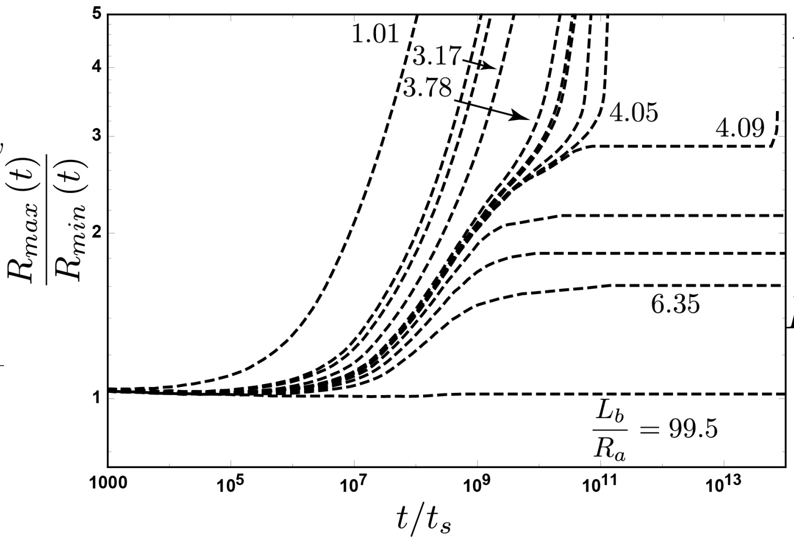

$t_s \equiv$ shut-in time

$R_{max} \equiv$ max distance to front

$R_{min} \equiv$ min distance to front

Birth of buoyant fracture in function of the fraction between the buoyancy lengthscale L_b (Lister & Kerr, 1991) and the radius of arrest for a pulse injection without buoyancy R_a.

$$R_a = \left(\frac{3}{\pi\sqrt{2}}\frac{E'V_o}{K'}\right)^{2/5} \qquad L_b = \left(\frac{K'}{\Delta\rho g}\right)^{2/3}$$

The limiting fraction is

$$L_b/R_a \approx 4.0$$

Plots to the left show simulations with PyFrac (Zia & Lecampion, 2019) for propagation (top) and arrest (bottom) normalized by the scales of Germanovich, Garagash, Murdoch & Robinowitz, (2014) (additional slides).

Large time solution

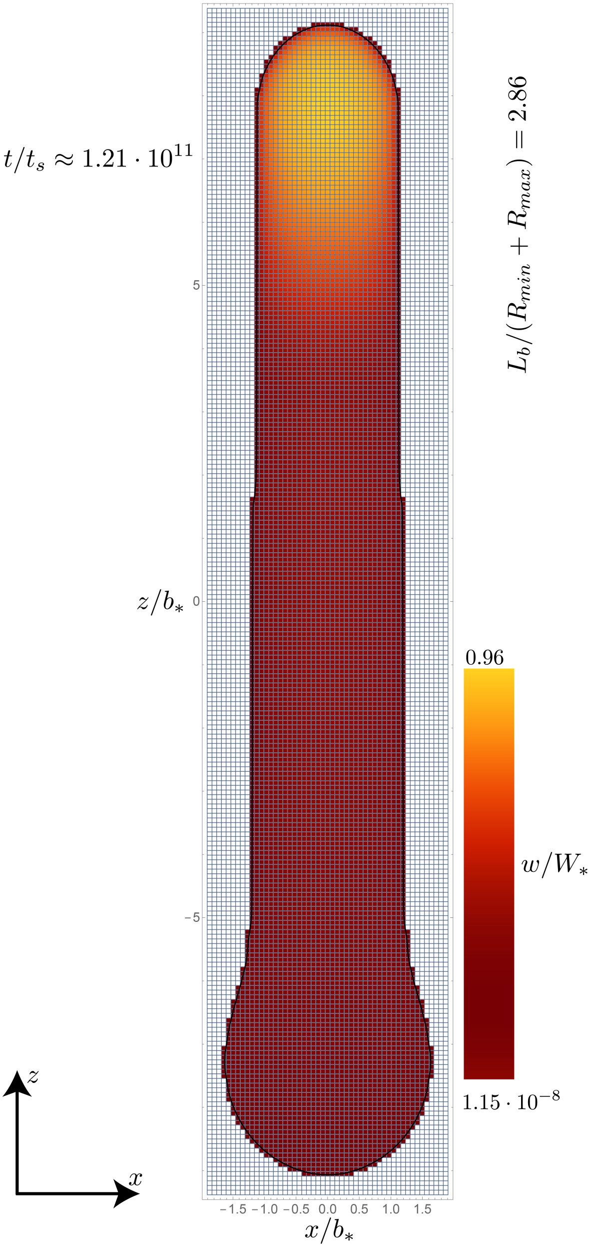

- At large time we approach the limiting solution of Germanovich *et al.*, (2014) for a finger-like dike propagation. The stable breadth

$$b_* \approx 2^{-8/3} L_b$$

is approached in our simulations to about 10%.

- The stable breadth is reached at times significantly larger than a characteristic timescale

$$t_{stab}^{[V]} \approx \frac{2^{15/2}}{3}\left(\frac{V_o E'}{\pi} - K' b_*^{5/2}\right)\frac{\mu' E'^2}{b_* K'^4}$$

Our simulations last up to $t \approx t_{stab}^{[V]} \cdot 10^3$.

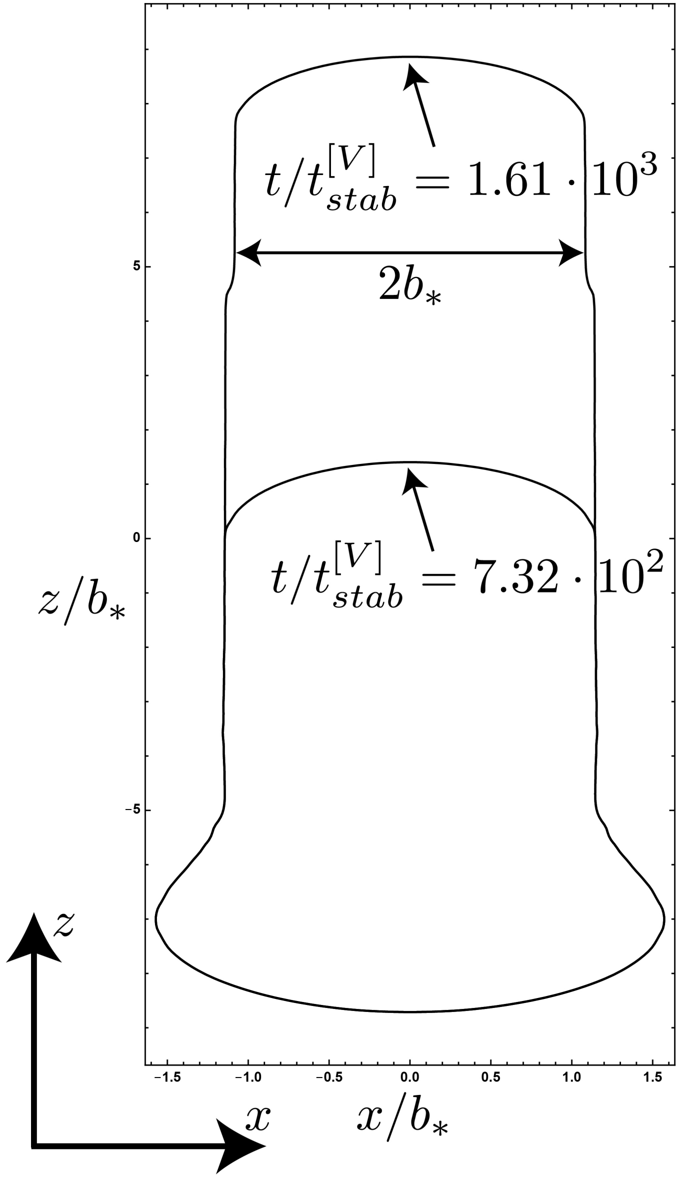

Fully-coupled 3D modelling of magmatic dike Propagation – finite pulse release from a point source

Andreas Möri[1,2], Brice Lecampion[1], Haseeb Zia[1]
[1]Ecole polytéchnique fédérale de Lausanne, Switzerland

Additional slides and Bibliography

EPFL

GeoEnergyLab

[2]Correspondence to: andreas.mori@epfl.ch

Further analysis

- Analysing the pressure profile (pressure gradient) and fluid flow inside the fracture to find the solutions of equilibrium shapes (e.g. analytical definition of the birth of dike propagation).
- Arrest is defined geometrically for now. We seek another definition in function of fluid flow.

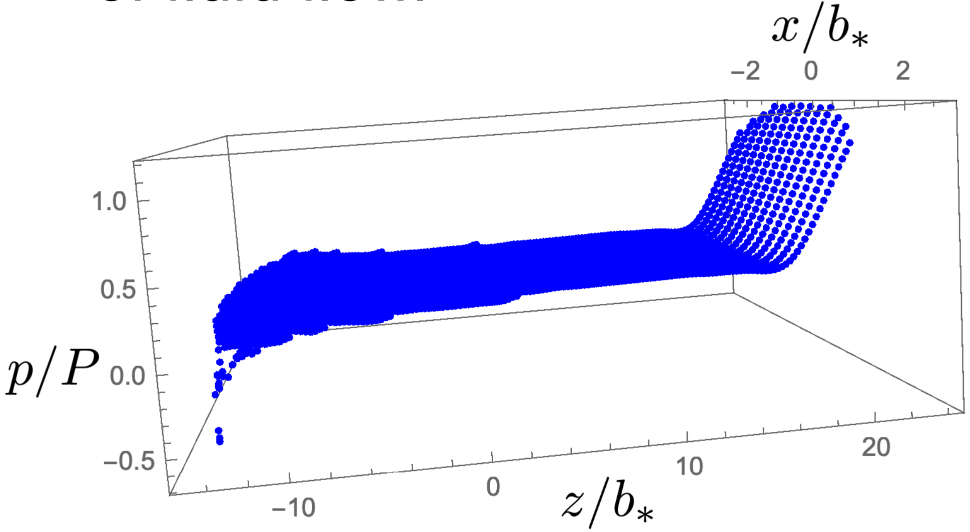

Dimensionless net pressure profile inside the fracture. The profile is constant along the breadth (along x). The head has a linear gradient along the vertical direction (z) as described in Germanovich et al., (2014). The normalized pressure gradient in the head found was approximately 0.25, which corresponds to a static solution inside the head. We recover this factor in our simulations up to 2% for dike propagation and exactly for fractures without buoyant propagation.

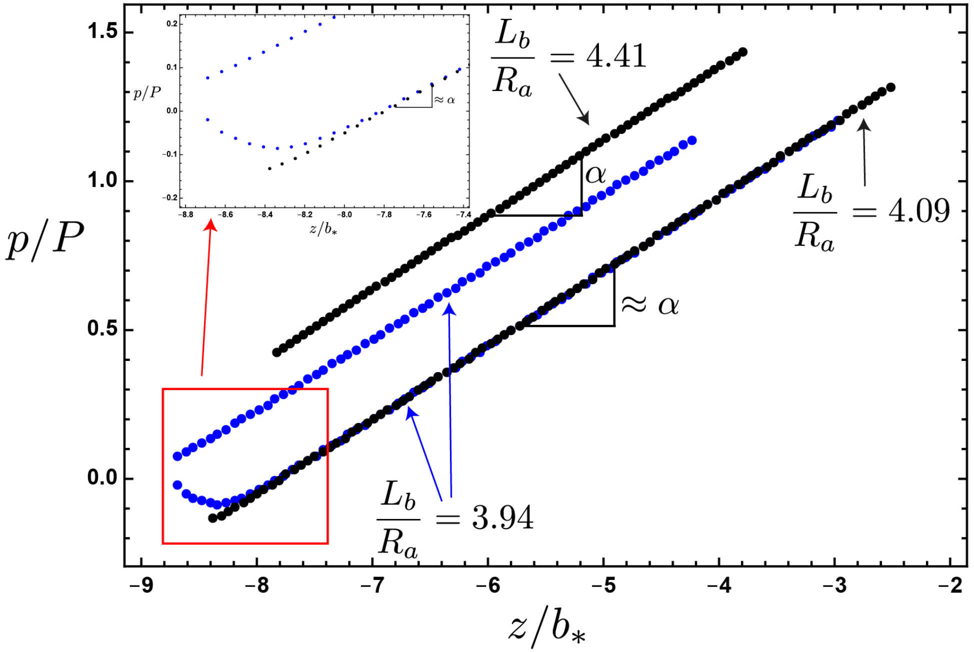

Normalized net pressure inside the fracture. For the black Simulations propagation stopped because equilibrium was reached. For the blue simulation some fluid flow remained allowing for buoyant propagation. Inset is a zoom on the not fully stabilized part.

Extension of the current work

- Focus on non-viscous shut-in.
- We expect a family of solutions to emerge in function of three dimensionless parameters

$$L_b/R_s,\ \mathcal{K}_s,\ L_b/R_a$$

  with R_s the radius at shut-in and $\mathcal{K}_s$ the dimensionless toughness at shut-in.
- Different combinations of those parameters may lead to a complicated parametric space.

Material parameters

- Alternative material parameters are defined following Detournay, (2016) (prime parameters) and Germanovich et al., (2014) (bar parameters)

$$E' = \frac{E}{1-\nu^2}, \quad K' = 4\sqrt{\frac{2}{\pi}}K_{Ic}, \quad \mu' = 12\mu$$

$$\bar{K} = \frac{1}{4}K', \; \bar{E} = \frac{1}{\pi}E', \; \bar{\mu} = \frac{\pi^2}{12}\mu'$$

- The scales used are the ones defined in Germanovich et al., (2014)

$$b_* \approx 2^{-8/3}L_b, \; W = \frac{\bar{K}\sqrt{b_*}}{\bar{E}}, \; P = \frac{\bar{K}}{\sqrt{b_*}}$$

Bibliography

Lister, J. R., & Kerr, R. C. (1991). Fluid- mechanical models of crack propagation and their application to magma transport in dykes. *Journal of Geophysical Research: Solid Earth*, *96*(B6):10049–10077.

Zia, H., & Lecampion, B. (2019). PyFrac: A planar 3D hydraulic fracture simulator, arXiv:1908.10788v2

Germanovich, L., Garagash, D. I., Murdoch, L., & Robinowitz, M. (2014). Gravity-driven hydraulic fractures. In *AGU Fall meeting.*

Detournay, E., (2016) Mechanics of Hydraulic Fractures, *Annual Review of Fluid Mechanics, 48,* pp. 311-339